

Relativistic effects on coronal ejection in variable X-ray sources

B. Mishra and W. Kluźniak

Nicolaus Copernicus Astronomical Center, Polish Academy of Sciences, ul. Bartycka 18, 00-716 Warszawa, Poland
e-mail:mbhupe@camk.edu.pl, wlodek@camk.edu.pl

Received ***; accepted ***

ABSTRACT

Context: Optically thin coronae around neutron stars suffering an X-ray burst can be ejected as a result of rapid increase in stellar luminosity. In general relativity (GR), radiation pressure from the central luminous star counteracts gravitational attraction more strongly than in Newtonian physics. However, motion near the neutron star is very effectively impeded by the radiation field.

Results: We discuss coronal ejection in a general relativistic calculation of the motion of a test particle in a spherically symmetric radiation field. At every radial distance from the star larger than that of the ISCO, and any initial luminosity of the star, there exists a luminosity change which leads to coronal ejection. The luminosity required to eject from the system the inner parts of the optically thin neutron-star corona is very high in the presence of radiation drag and always close to the Eddington luminosity. Outer parts of the corona, at a distance of $20 R_G$ or more, will be ejected by a sub-Eddington outburst. Mildly fluctuating luminosity will lead to dissipation in the plasma and may explain the observed X-ray temperatures of coronae in low mass X-ray binaries (LMXBs). At large radial distances from the star ($3 \cdot 10^3 R_G$ or more) the results do not depend on whether or not Poynting-Robertson drag is included in the calculation.

Key words. stars: neutron – stars: winds, outflows – X-rays: binaries – scattering – accretion, accretion disks

1. Introduction

Most LMXBs vary in luminosity on many timescales. Particularly rapid and luminous variations are exhibited by the numerous X-ray bursters, which are thought to be neutron stars undergoing a thermonuclear explosion on their surface, yielding an Eddington luminosity at maximum. Sometimes the maximum flux corresponds to super-Eddington luminosities, as in the pulsating neutron star “LMC transient” A0535-668 (at a firm distance of 50 Kpc), which is thought to attain an isotropic flux $L_\infty = 1.2 \times 10^{39}$ erg/s = $6.9 L_{\text{Edd}}$ for a $1.4 M_\odot$ star (Bradt et al. 1983). One may ask whether the variability of X-ray luminosity has any influence on the state of circumstellar matter.

The observed LMXBs are thought to be powered by accretion occurring through an optically thick disk. In this paper we are considering the response of accretion flows in the optically thin regions of the system to X-ray variability of the source. We are considering a corona in a variable X-ray source. In this context, corona means optically thin plasma “above the surface” of the disk. The effects of luminosity change on the motion of optically thin accreting matter in Newtonian dynamics are already known, an impulsive increase in the stellar luminosity of the star may lead to coronal ejection if the luminosity is increased by one half or more of the difference between Eddington luminosity and the initial one (Kluźniak 2013). However, that result was derived analytically taking no account of radiation drag. Walker & Meszaros (1989) pointed out the effect of Poynting-Robertson drag (Robertson 1937) for accretion flows around high luminosity neutron stars. Proper inclusion of radiation drag requires a numerical solution in general relativity (GR), and we are presenting such solutions in this paper. Recently, Stahl et al. (2013) discussed the problem for super-Eddington outbursts in initially non-radiating stars. Here, we consider a wide range of initial and final luminosities.

We are attempting to understand luminosity effects on the corona by modeling test-particle motion around the star. The dynamics are described by equations of motion of a particle moving in a spherically symmetric radiation field in the Schwarzschild metric, while interaction with the radiation by momentum absorption with a cross-section whose numerical value will correspond to the Thomson cross-section times the mass of the particle expressed in units of proton mass. This assures that the conventional Eddington luminosity, L_{Edd} , will balance gravity exactly for hydrogen plasma at infinity (i.e., in the Newtonian limit). The calculation can be carried over to other compositions, and other cross-sections for photon absorption, by suitably re-defining the Eddington luminosity.

The radiation, assumed to be originating on the surface of a neutron star, will have two important effects on the motion: first, it will counteract gravity by transferring the radial component of (a part of) its momentum; second, it will exert a drag on the moving particle. The calculation is performed in GR, and includes all non-vanishing components of the radiation stress tensor.

The paper is organized in the following manner. In § 2 we shall briefly explain the equations of motion that describe the trajectories of test particles. In § 3.1, in order to isolate the gravitational effects of GR, we shall present results of a simplified calculation without radiation drag, and in § 3.2 we will describe the test particle behavior determined from the complete equations of motion (e.o.m.), which include radiation drag. In § 4 we discuss the results and present the conclusions in § 5.

2. Equations of motion

We performed all the calculations in the Schwarzschild metric, using spherical polar coordinates (r, θ, ϕ) . For a spherically symmetric radiation field, motion of a test-particle is restricted

to one plane and we choose it to be the equatorial plane ($\theta = \pi/2$). Abramowicz et al. (1990) performed a rigorous analysis of purely radial motion of a test particle in the combined gravity and isotropic radiation fields of a spherical, non-rotating, compact star, and we shall use their stress energy tensor of radiation, $T^{(\mu)(\nu)}$, calculated in a stationary observer's tetrad assuming isotropic emission from the surface of star, see also Stahl et al. (2013). Numerical solutions of the equations of motion of test particle trajectories in a steady radiation field have been obtained e.g., by Bini et al. (2009) and Stahl et al. (2012) in the Schwarzschild metric, and by Oh et al. (2010); Bini et al. (2011) in the Kerr metric.

To describe in detail the effects of *variable luminosity* on the motion of optically thin plasma, and specifically the effects of impulsive changes in luminosity on test-particle trajectories, we use two sets of equations in the present paper. One, a simplified set, describes the trajectories of test particle without considering radiation drag, and the other includes all components of the radiation stress tensor, including the terms responsible for radiation drag.

2.1. Complete equations of motion ("with drag")

We performed the computations using dimensionless coordinates scaled by gravitational radius R_G , i.e., the dimensionless radial position, x , stellar radius, X , and proper time, τ ,

$$d\tau = \frac{ds}{R_G}, \quad x = \frac{r}{R_G}, \quad X = \frac{R}{R_G},$$

where the gravitational radius is $R_G = GM/c^2$. It is convenient to abbreviate the metric coefficient as $B = (1 - 2/x)$. The e.o.m. are (e.g., Stahl et al. 2012, 2013)

$$\frac{d^2x}{d\tau^2} = \frac{k}{\pi I(R)X^2} \left(BT^{(r)(t)}u^t - \left[T^{(r)(t)} + \varepsilon \right] \frac{dx}{d\tau} \right) + \quad (1)$$

$$+ (x-3) \left(\frac{d\phi}{d\tau} \right)^2 - \frac{1}{x^2},$$

$$\frac{d^2\phi}{d\tau^2} = -\frac{d\phi}{d\tau} \left(\frac{k}{\pi I(R)X^2} \left[T^{(\phi)(\phi)} + \varepsilon \right] + \frac{2}{x} \frac{dx}{d\tau} \right), \quad (2)$$

where

$$\varepsilon = BT^{(t)(t)}(u^t)^2 + B^{-1}T^{(r)(r)} \left(\frac{dx}{d\tau} \right)^2 + \quad (3)$$

$$+ x^2 T^{(\phi)(\phi)} \left(\frac{d\phi}{d\tau} \right)^2 - 2T^{(r)(t)}u^t \frac{dx}{d\tau}, \quad (4)$$

and the time component of the particle four velocity is given by

$$u^t = B^{-\frac{1}{2}} \left[1 + B^{-1} \left(\frac{dx}{d\tau} \right)^2 + x^2 \left(\frac{d\phi}{d\tau} \right)^2 \right]^{\frac{1}{2}}. \quad (5)$$

In all the computations the luminosity at the surface of the star, $L(R)$, is represented in units of Eddington luminosity as k (Eqs. 1, 2). One can also display the results in terms of the luminosity at infinity, L_∞ . These are related through

$$k = \frac{L(R)}{L_{\text{Edd}}} = \frac{L_\infty}{L_{\text{Edd}}} \left(1 - \frac{2}{R} \right)^{-1}. \quad (6)$$

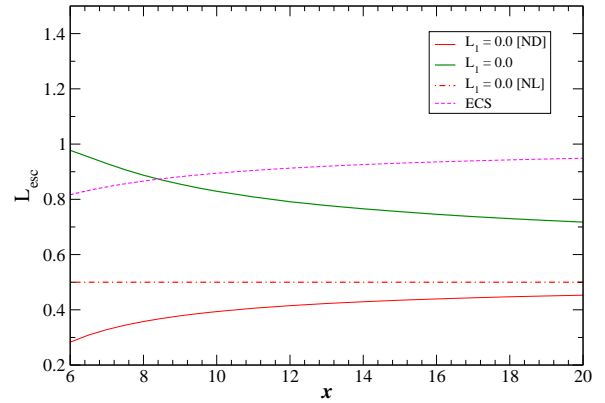


Fig. 1. Minimum luminosity that will eject to infinity a particle initially in circular orbit at x . Plot compares solutions of the full e.o.m. (solid green curve, Eqs. 1, 2) with solutions of the simplified equations that neglect the effects of radiation drag (“[ND]” thin red line, Eqs. 7, 8). Initial luminosity is $L_1 = 0$, stellar radius $X = 5$. The Newtonian limit is also shown (dot-dashed line), as well as the radius of the Eddington capture sphere (ECS). See text for details.

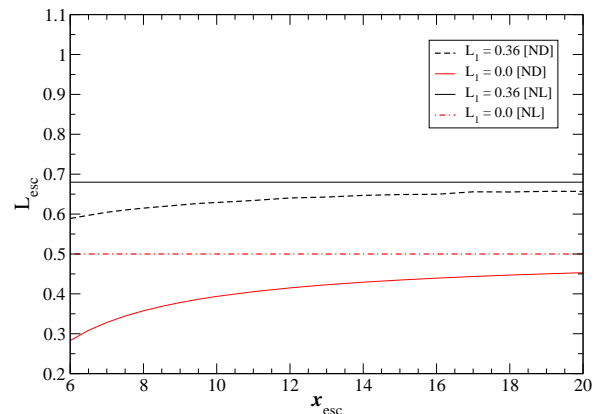


Fig. 2. Radius of the escape sphere when drag is neglected. The minimum luminosity, L_{esc} , that unbinds a particle in circular orbit at x_{esc} is shown as a function of the initial orbital radius, for two values of initial luminosity, $L_1 = 0.0$, and 0.36 . Stellar radius is $X = 5.0$. Constant L_{esc} lines represent Newtonian limits (NL) for $L_1 = 0.0, 0.36$. If there were no drag, particles from all circular orbits of radii in the range $6 \leq x(0) < x_{\text{esc}}(L_{\text{esc}})$ would escape the system, and the initial radius in the outgoing trajectory, $x(0)$, would be its periastron as well.

To obtain $x(\tau)$ and $\phi(\tau)$ we integrated Eq. 1 and Eq. 2 using the code of Stahl et al. (2012) and Wielgus et al. (2012), relying on the Dormand-Prince method, which is a fourth-order accuracy, adaptive step-size Runge-Kutta type integration method. In all our simulations we assumed a fixed radius of neutron star of $X = 5$. At this stellar radius, the marginally stable radius (ISCO) is outside the surface of the neutron star (Kluźniak & Wagoner 1985).

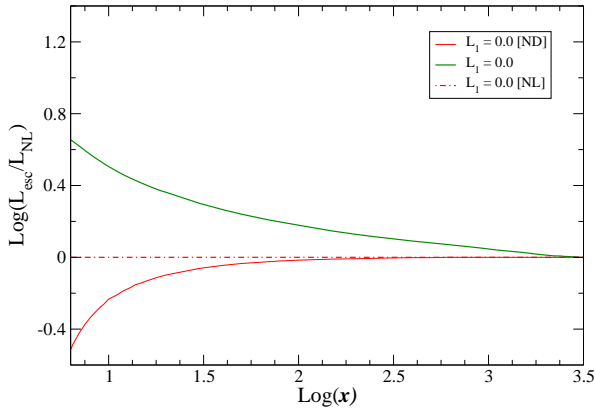


Fig. 3. Plot shows convergence of results using Eqs. 1, 2 and Eqs. 6, 7, with the Newtonian limit. The ratio is plotted of the minimum luminosity sufficient to unbind a particle, initially in a circular GR orbit at $L_1 = 0$, to the corresponding value in the Newtonian limit. Uppermost (thick green) curve corresponds to Eqs. 1 and 2, and red continuous curve to Eqs. 7 and 8.

2.2. Equations of motion without drag

Neglecting the terms responsible for radiation drag, one obtains simplified equations of motion involving only one component of the radiation stress tensor,

$$\frac{d^2x}{d\tau^2} = \frac{k}{\pi I(R)X^2} BT^{(r)(t)} u^t + (x-3) \left(\frac{d\phi}{d\tau} \right)^2 - \frac{1}{x^2}, \quad (7)$$

$$\frac{d^2\phi}{d\tau^2} = -\frac{d\phi}{d\tau} \left(\frac{2}{x} \frac{dx}{d\tau} \right). \quad (8)$$

3. Coronal ejection

If a particle is moving in a circular orbit, it can become unbound under a sudden increase of luminosity. For a test particle in Newtonian dynamics, moving initially in a Keplerian circular orbit under initial luminosity L_1 , the minimum luminosity change required to unbind the particle is $(L_{\text{Edd}} - L_1)/2$. Such a luminosity change will also lead to coronal ejection if the radiation drag is neglected Kluzniak (2013).

We will be contrasting conditions under which particles escape to infinity with those in which the particles remain in the system. The results presented below are based on numerical solutions for the trajectories. Therefore, we need a numerical criterion for deciding which outgoing trajectories are bounded, and which ones are unbounded. We adopted one¹ in which we computed the Newtonian effective specific energy of the test particle at $x = 3000$. By the effective specific energy we mean the specific energy in the potential $-GM_{\text{eff}}/r$, with $M_{\text{eff}} = M(1 - L_{\infty}/L_{\text{Edd}})$; this prescription takes account of the radial radiation pressure term. If the Newtonian effective specific energy is positive at $x = 3000$, the trajectory is deemed to be unbounded (i.e., extending to infinity), and if it is negative, the trajectory is deemed bounded. In practice, at such a large distance the trajectory of those particles which have reached it is always very nearly radial, and the influence of drag is negligible there.

¹ This criterion differs in some respects from the one adopted by Stahl et al. (2013).

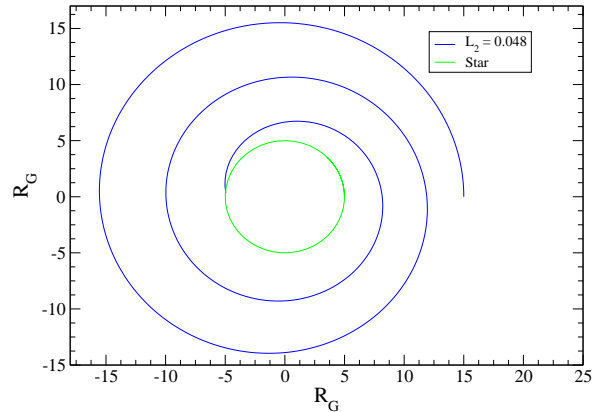


Fig. 4. Plot shows test-particle trajectory for a constant $L = 0.048$. Instead of maintaining a circular orbit the test particle follows a spiral trajectory and accretes on the surface of star.

To isolate the effects of drag from gravitational effects in GR we shall discuss two cases, in the first case we shall omit effects of radiation drag (Eqs. 7, 8), and in the second case we shall use the complete e.o.m. (Eqs. 1, 2) that include also the radiation drag terms. Our results show convergence of the two cases at large radii (Fig. 3). Interestingly, radiation drag dominates GR corrections, and already at a radius of about $10^2 R_G$ the non-drag GR corrections appear to be negligible. At $r = 10^3 R_G$ the fully relativistic solution (including drag) differs from the Newtonian limit by just a few per cent.

In the following we give the value of luminosities at infinity scaled by the Eddington luminosity. Thus, a “luminosity of L_1 ” signifies $L_{\infty} = L_1 L_{\text{Edd}}$.

3.1. GR effects without drag

We consider an initial luminosity, L_1 which at some point in the evolution of the system will be changed impulsively to a different value L_2 . In this subsection we assume the absence of radiation drag. Thus a test particle can move in a Keplerian orbit at a fixed radial distance from the star, as long as the luminosity is held fixed. It will continue to move on nearby orbits under very small changes in the luminosity. But if the luminosity change is large enough, the particle can escape the system.

We investigate for what luminosity change $L_2 - L_1$ the particle will become unbound (neglecting radiation drag). The initial conditions correspond to a circular orbit, at a particular radius around the star of luminosity L_1 . To find the trajectory we integrate Eqs. 7, 8. Since the effective radiative force diminishes more rapidly with increasing distance from the center of a variable X-ray source than the gravitational attraction, in the absence of drag a smaller luminosity change is required to eject the particle from a circular orbit close to the ISCO ($x = 6$ for a non-rotating neutron star) than from a more distant one. This is clear in Fig. 2. The plotted value, $L_{\text{esc}}(x_{\text{esc}})$, corresponds to the minimum luminosity change $L_{\text{esc}} - L_1$ sufficient to unbind a particle that was in a circular orbit at $x = x_{\text{esc}}$ at luminosity L_1 , assuming that drag is neglected. Also shown (constant L_{esc} lines in the figure) is the corresponding Newtonian limit of Kluzniak (2013).

It turns out that for any given pair of initial and final luminosities there is a sphere, inside of which the luminosity change is sufficiently large for all orbits to become unbounded—all particles within the sphere abandon their previously stable circular orbits for trajectories extending to infinity. On the other hand,

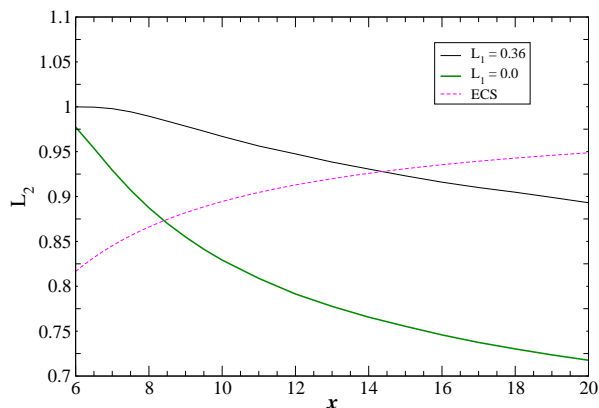


Fig. 5. The continuous curves show the variation with the final luminosity of minimum escape radius, $x = x_{\text{esc}}(L_2)$, after a sudden change to L_2 from $L_1 = 0$, or 0.36. The same curves also show the minimum final luminosity, $L_2 = L_{\text{esc}}(x)$ required to eject to infinity a particle previously orbiting at x . Stellar radius is $X = 5.0$. Dotted curve represents the variation of ECS radius with L_2 (see text).

particles previously orbiting outside the sphere remain bound. We will denote the radius of this *escape sphere* by x_{esc} . Another way of looking at Fig. 2 is that it presents the escape sphere radii (in motion without drag) as a function of the final luminosity L_{esc} , for two different initial luminosities.

3.2. GR effects with drag

Now we shall integrate Eq. 1 and Eq. 2 to compute the trajectories of test particles suffering the influence of the full radiation tensor. Radiation drag is automatically included in the formalism, and the angular momentum and energy of the test particle are no longer constants of motion—in this case we cannot get an analytical expression like in Newtonian dynamics by integrating the equations. In a steady radiation field, a circular orbit cannot be maintained—drag will cause the orbiting test particle to lose angular momentum and energy, and will cause it to follow a spiral trajectory (Walker & Meszaros 1989), cf. Fig. 4.

If initially a test particle is moving under the influence of luminosity L_1 , a sudden change to a different luminosity L_2 will change its trajectory. For an initially non-luminous star ($L_1 = 0$) the discussion is straightforward. The initial trajectory may be taken to correspond to a stable circular orbit, and the parameter k in Eqs. 1 and 2 and may be taken to be non-zero starting at any moment. Again, for any radius of the initial circular orbit, there is a minimum luminosity $L_2 = L_{\text{esc}}$ which makes the test-particle unbound (Fig. 1). Note that now L_{esc} is a monotonically decreasing function of x . For comparison, also plotted in Fig. 1 are L_{esc} in the Newtonian limit (dot-dashed curve, Kluźniak 2013), and in the GR calculation with radiation drag neglected (Eqs. 7, 8 and § 3.1). Also shown (magenta dashed curve) is the effective Eddington luminosity, $L_{\text{eff}}(x)$, i.e., that luminosity² at which a test particle located at x may be in a static equilibrium (Phinney 1987). The inverse function $x(L_{\text{eff}})$ gives the radius of the Eddington capture sphere (Stahl et al. 2012, 2013), discussed below.

In the general case ($L_1 \neq 0$), the choice of initial conditions is less obvious. Since we are interested in the change of the motion of accretion disk corona, resulting from the change in luminos-

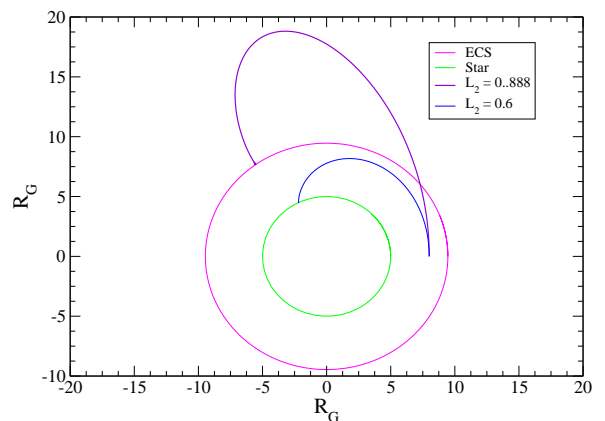


Fig. 6. Two qualitatively different trajectories with the same initial condition for two different luminosities: $L_2 = 0.6$ (thin blue trajectory) and $L_2 = 0.888$ (violet trajectory). For $L_2 = 0.888$ an ECS is present at $x_{\text{esc}} = 9.44$. The radius of star $X = 5.0$. The initial conditions are taken for $x = 8.0$ and $L_1 = 0.36$ (cf. Fig. 5.)

ity, we consider initially circular orbits. The initial condition for our calculations corresponds to the motion of a test particle instantaneously in a circular orbit appropriate for stellar luminosity L_1 . Effectively, we assume that in a steady luminosity field the system will adjust to the presence of radiation drag, resulting in nearly circular motion of the accreting fluid.

Imagine a particle executing a circular orbit around the star when it shines with luminosity L_1 . This would only be possible if some external agency (e.g., the accretion disk) continually replenished the angular momentum and energy lost to radiation drag. The star is assumed to impulsively change its luminosity to L_2 . We imagine the external agency to cease operation precisely at that instant when the spherical wavefront corresponding to the change in luminosity arrives at the orbit (for instance, the coupling between the disc and the corona is disrupted by the additional radiation pressure). Future hydrodynamic calculations will no doubt elucidate the true state of affair—ours is an exploratory calculation aiming to qualitatively identify the main features in the response of a corona to variable illumination by the central star.

Technically, we integrated Eq. 1 and Eq. 2 with a value of k corresponding to the final luminosity, with the initial condition corresponding to a radius and velocity of a circular-orbit solution of Eqs. 7 and 8 at luminosity L_1 . The particle then follows a trajectory defined by its initial velocity and position, as well as the three stellar parameters M, R, L_2 .

Again, we find that at any particular radius, x , there is a minimum luminosity $L_2 = L_{\text{esc}}$ that will cause a particle satisfying the initial conditions to escape to infinity. A final luminosity value larger than L_{esc} will also lead to the expulsion of the particle. The $L_{\text{esc}}(x)$ curve is monotonically decreasing. Fig. 5 illustrates this behavior. The inverse function, $x_{\text{esc}}(L_2) = x(L_{\text{esc}})$ is the minimum radius of circular orbits from which the particles escape (*minimum escape radius*), for a given value of L_2 . For a given value of L_2 , the sphere at x_{esc} now divides space into an outer region, $x \geq x_{\text{esc}}$, from which the particles escape, and an inner region, $x < x_{\text{esc}}$, the particles from which remain bound to the system (although they may leave the region $x < x_{\text{esc}}$).

Clearly, radiation drag is responsible for capturing all particles that are initially within the sphere of escape radius x_{esc} . At lower luminosities, the particles will actually be accreted onto the central star. However, at about Eddington luminosities they

² $L_{\text{eff}}(x) = (1 - 2/x)^{1/2}$.

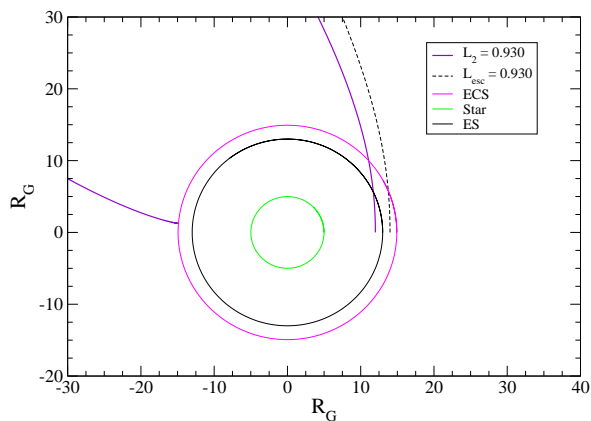


Fig. 7. Figure shows trajectories corresponding to the $L_1 = 0.36$ curve in Fig. 5. $L_2 = 0.930$ is fixed in both trajectories. The stellar surface is shown at $X = 5.0$, and the ECS at $x_{ECS} = 14.927$ (magenta), the minimum escape radius is $x_{esc} = 13.0$ (middle circle in black). Bounded (solid violet line) trajectory starts at $x = 12.0$, unbounded (black dashed) trajectory starts at $x = 14.0$.

will lose all their momentum before settling on the star, and will levitate above the surface of the star in a state of equilibrium on a spherical surface concentric with the star, the so called *Eddington capture sphere* (ECS) (Stahl et al. 2012, 2013). The ECS exists at $X \leq x < \infty$ for luminosity L when $L_{eff}(x) = L$ (cf. footnotes 2 and 3).

This is illustrated in Fig. 6, where two trajectories are shown for motion starting with the same initial condition (instantaneously circular orbit at $x = 8$ under luminosity $L_1 = 0.36$), but occurring for two different values of luminosities L_2 , both satisfying $L_2 < L_{esc}(x)$, so that both motions are bounded. The two trajectories differ qualitatively in their termination point: at final luminosity $L_2 = 0.6$ the particle is accreted with nonzero velocity onto the surface of the star, while at $L_2 = 0.888$ the ECS is present, on which the non-escaping particles come to rest. The latter case is an example of particles being trapped outside their initial position, radiation drag causing here a net displacement outwards, somewhat paradoxically. The ECS luminosity-radius relation is shown in Fig. 5. The quasi-paradoxical net displacement outwards occurs only for radii to the left of the intersection of the ECS curve with the $L_{esc}(x)$ curve, and only for values of L_2 between the two curves. In Fig. 5 the minimum escape radius has been presented for simulations with two values of initial luminosity, $L_1 = 0.0$ and 0.36 . We also plotted variation of ECS radius with the final luminosity, L_2 . For a fixed initial luminosity L_1 , the escape sphere and the ECS coincide at a particular radius (Stahl et al., 2013). In Fig. 5 for initial luminosity $L_1 = 0.0$ and 0.36 , the minimum escape radius and the ECS radius are the same at $x_{esc} = 8.412$ and 14.365 , and corresponding luminosities $L_2 = 0.873$ and 0.928 , respectively.

Fig. 7 is helpful in illustrating the concepts of the minimum escape radius x_{esc} , and of the ECS. Here, we started with an initial luminosity of $L_1 = 0.36$, impulsively changed to $L_2 = 0.930$. Two trajectories are illustrated tangent to circles of radii $x_1 = 12.0$ and $x_2 = 14.0$. The initial velocities correspond to instantaneously circular motion under the influence of $L_1 = 0.36$, as described above. In this example the minimum escape radius is $x_{esc} = 13.0$, and clearly $x_1 < x_{esc}$, while $x_2 > x_{esc}$. In the latter case [$x(0) = x_2$] the particle enters an escaping trajectory under the impulsive change of luminosity, while in the former [$x(0) = x_1$] it is captured by the ECS at $x = 14.927$.

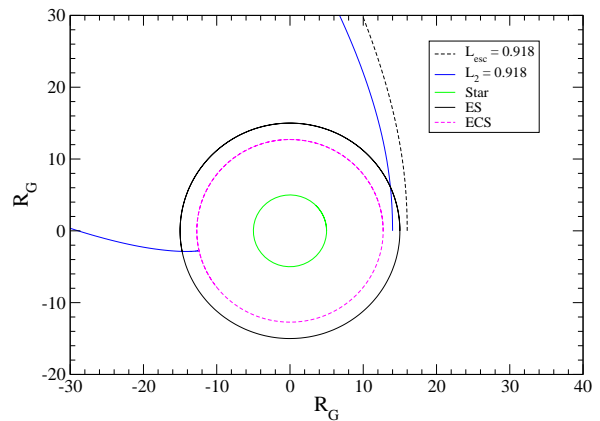


Fig. 8. Trajectories corresponding to the $L_1 = 0.36$ curve in Fig. 5 for $L_2 = 0.918$. Black dashed trajectory is unbounded. The bounded trajectory (blue) ends on an ECS, which in this case is within the sphere of minimum escape radius (black circle).

Two non-overlapping trajectories for the case of nonzero initial luminosity ($L_1 = 0.36$) are illustrated in Fig. 8. The final luminosity is taken to be $L_2 = 0.918$, and now the ECS is inside the sphere of minimum escape radius. The black dashed trajectory illustrates an unbounded trajectory starting from an instantaneously circular orbit of radius exceeding x_{esc} . The test particle on the blue continuous trajectory is captured on the ECS. If the final luminosity is smaller than the one corresponding to an ECS at the stellar radius (at $X = 5$), the non-escaping particles (i.e., ones with $x(0) < x_{esc}$) will accrete on the star.³

4. Discussion

Radiation increases so strongly towards the source in general relativity that at first sight it seems easy to unbind matter orbiting a compact luminous star. For instance, a modest increase in luminosity would be sufficient to expel matter from the ISCO *if there were no radiation drag*, e.g., a change from 0 to $0.283 L_{Edd}$, or from $0.360 L_{Edd}$ to $0.589 L_{Edd}$ would suffice, as can be seen in Fig. 2. However, the same radiation very strongly impedes the motion of matter moving in the optically thin regions illuminated by the star by exerting a drag that reduces the angular momentum and energy inherent in the motion. When this effect is properly taken into account, the conclusion is reversed: it is, in fact, very difficult to expel matter orbiting at the ISCO, typically this is only possible when super-Eddington luminosities are attained. However, the effects of drag fall off very quickly with distance to the radiation source, so that an Eddington outburst of a lower luminosity source (say, initial luminosity $< 0.3 L_{Edd}$), such as an atoll source is sufficient to clear out all test particles orbiting in the optically thin region at $r \gtrsim 10 R_G$ (Figs. 1,5)

The numerical results obtained in the paper apply to the motion of test particles. However, they should be also applicable, at least qualitatively, to optically thin plasma, e.g., the coronae of accretion disks. The radiation front following an outburst of the source moves at the speed of light appropriate for the medium, which is always larger than both the sound speed and the speed of the orbiting particles along any trajectory they may follow. All parts of the optically thin plasma will feel the influence of radiation before any significant hydrodynamic interaction occurs

³ The ECS radius ranges from R to infinity for luminosity in the range $\sqrt{1 - 2R_G/R} \leq L_\infty/L_{Edd} < 1$ (Stahl et al. 2013).

between the different regions at various radial distance from the source.

First let us consider plasma outside the spherical surface of minimum escape radius. Assuming that the plasma is distributed axisymmetrically, we can rule out intersection of outgoing trajectories from a ring of plasma originally located at a given radial distance from the source. Further, as the effects of drag fall off with distance, the motion of the outer rings of plasma will not be impeded by that of the inner rings. However, it is true that the inner rings will at first travel faster than the outer rings, because the outward velocity shortly after the passage of the radiation front scales with initial orbital velocity. This will lead to compressive heating of the plasma, thus robbing it of some kinetic energy and making the escape of the plasma less likely. The expected effect of replacing test particles with plasma is to increase the minimum luminosity change required to make the trajectories unbounded or, equivalently, to increase the minimum escape radius x_{esc} for a given final luminosity.

By the same arguments, plasma will remain bound to the system in those regions from which test particles cannot escape. Thus, we arrive at a robust conclusion that even in Eddington luminosity outbursts radiation drag makes it difficult for matter orbiting near the ISCO to escape the system. However, that region will be temporarily cleared of any optically thin plasma while the plasma follows the initial outwards-going part of its bounded trajectory.

As we have seen in Figs. 6, 7, 8, the bounded trajectories can cover a wide range of distance. It seems obvious that under the conditions corresponding to the non-circular bounded trajectories discussed in this paper, colliding shells of plasma will undergo compressive and dissipative heating. The temperatures involved are expected to be quite high, a fraction of the virial energy being involved in the transfer of kinetic to thermal energy (Kluźniak 2013). Thus, we would like to suggest that strong illumination alone of optically thin plasma may provide a sufficient heating mechanism to explain the origin of the observed high temperatures in the X-ray emitting coronae of LMXBs.

5. Conclusions

We have numerically solved in full GR the equations of motion of a test particle moving in a strong radiation field. The motion of test particles, and most likely also of plasma, around a gravitating luminous body is strongly affected by rapid changes of its luminosity. For any initial luminosity and circular orbit, a sufficiently large increase in luminosity will unbind the particle. The effects of GR, and especially of radiation drag, make this “escape” luminosity a strong function of distance for the first several tens of gravitational radii. This GR result is in contrast with the Newtonian case, where the escape luminosity is independent of radius.

In particular, close to the ISCO radiation drag is so strong, that it takes an about Eddington luminosity outburst to eject particles to infinity. If the initial luminosity is a sizable fraction of Eddington the final luminosity required to eject the particle may be super-Eddington. This may explain why X-ray bursters typically seem to be rebuilding their inner accretion disks shortly after the outburst. However, the effects of radiation drag drop very rapidly with distance, and already at radii $\sim 20R_G$ a sub-Eddington burst is typically sufficient to eject test particles to infinity.

We expect that similar conclusions will also hold for the motion of plasma, or hot gas, and we intend to verify these expectations in future work with a hydro code.

Acknowledgements. We thank Wenfei Yu for illuminating conversations in the early stages of this project. Research supported in part by Polish NCN grant UMO-34 2011/01/B/ST9/05439.

References

- Abramowicz, M. A., Ellis, G. F. R., & Lanza, A. 1990, *ApJ*, 361, 470
 Bini, D., Jantzen, R. T., & Stella, L. 2009, *Classical and Quantum Gravity*, 26, 055009
 Bini, D., Geralico, A., Jantzen, R. T., Semerák, O., & Stella, L. 2011, *Class. Q. Grav.*, 28, 035008
 Bradt, H.V.D., McClintock, J.E., 1983, *ARAA*, 21, 13
 Kluźniak, W. 2013, *A&A*, 551, A70
 Kluźniak, W., Wagoner, R.V. 1985, *ApJ*, 297, 548
 Oh, J. S., Kim, H., & Lee, H. M. 2010, *Phys. Rev. D*, 81, 084005
 Phinney, E. S. 1987, in *Superluminal Radio Sources*, eds. J. A. Zensus, & T. J. Pearson (Cambridge: Cambridge University Press), 12
 Robertson, H. P. 1937, *MNRAS*, 97, 423
 Stahl, A., Kluźniak, W., Wielgus, M., & Abramowicz, M., 2013, *A&A*, in press
 Stahl, A., Wielgus, M., Abramowicz, M., Kluźniak, W., & Yu, W. 2012, *A&A*, 546, A54
 Walker, M. A. & Meszaros, P. 1989, *ApJ*, 346, 844
 Wielgus, M., Stahl, A., Abramowicz, M., & Kluźniak, W. 2012, *A&A*, 545, A123